Cement & Concrete Composites 33 (2011) 328–333

Contents lists available at ScienceDirect

Cement & Concrete Composites

journal homepage: www.elsevier.com/locate/cemconcomp

Strengthening effects of DFRCC layers applied to RC flexural members

S.K. Shin [a], K. Kim [b], Y.M. Lim [b,*]

[a] Research Institute of Technology, Hanwha Engineering & Construction, 6 ShinsungDong YousungGu, Daejeon 305-345, Republic of Korea
[b] School of Civil & Environmental Engineering, College of Engineering, Yonsei University, Seoul 120-749, Republic of Korea

ARTICLE INFO

Article history:
Received 9 March 2009
Received in revised form 31 August 2010
Accepted 3 September 2010
Available online 8 September 2010

Keywords:
Ductile Fiber Reinforced Cementitious Composite (DFRCC)
Strain capacity
Strengthening effect
Discrete model

ABSTRACT

Ductile Fiber Reinforced Cementitious Composite (DFRCC) features a superior strain capacity of 5–6% under tensile loading. However, the strengthening effect of DFRCC on the flexural performance of RC beams is not clearly understood at present. In this study, we numerically investigate the DFRCC strengthening effect as applied to the tension region of RC beams. More specifically, numerical simulations are carried out for four-point bending RC beams strengthened with a cover thickness of DFRCC and with twice the cover thickness at the bottom tension section of the composite beam. To determine the effects of strain capacity and the strain-hardening slope of DFRCC, numerical simulations are carried out with DFRCC strain capacities ranging from 1% to 5%. From these studies, it is shown that the load carrying capacity and displacement at failure are influenced by the strain capacity and strain-hardening slope of DFRCC, but not to a significant degree. DFRCC strengthening on a tension zone can reduce both stress levels and stress concentrations in the reinforcement and can reduce crack width. It also can delay flexural failure of the structure due to the damage-tolerant behavior of DFRCC.

1. Introduction

The stiffness of RC beams is decreased due to various causes such as concrete cracking and reinforcement corrosion [1–3]. In order to prevent the durability of structures from degrading, older structures require periodic maintenance. From an economic point of view, efforts to repair or strengthen structures are preferable to reconstructing them [4]. It has been shown that one successful reinforcement method is to bond a steel plate, FRP sheet, or other material to the tension faces of structural members. In these cases, compatibility between the concrete and the repair material is the most important factor in selecting a repair material [5,6]. Cement-based materials are suitable for repairing RC structures due to the match between their mechanical and physical properties (e.g., coefficient of thermal expansion, fracture energy, and permeability), as well as other important considerations, such as cost, availability, and constructability [7–9].

Recently, Ductile Fiber Reinforced Cementitious Composite (DFRCC) or Strain Hardening Cementitious Composite (SHCC) has been developed as a repair material for RC structures [10–16]. DFRCC/SHCC is a cement-based material with strain-hardening behavior and a high tensile strain capacity. It also has a superior fracture resistance capacity [15]. The ultimate tensile strength and strain capacities can be as high as 5.0 MPa and 5–6%, respectively. When loading is applied to an RC member repaired with DFRCC/SHCC, more numerous but thinner cracks are expected to form on the beam tension face, in contrast to the fewer but wider cracks of an ordinary RC beam. More numerous finer cracks are expected to reduce stress concentrations and result in a more efficient stress distribution across the tension face.

In the authors' previous paper [6], the strengthening effect of DFRCC/SHCC applied to the tension region of plain concrete beams was both numerically and experimentally examined. In the present work, investigations focus on the flexural behavior of an RC beam repaired with DFRCC/SHCC on the tension face. RC beams with different repair thicknesses and strain capacities of DFRCC/SHCC are simulated in order to assess the strengthening effects and failure modes. For the numerical simulations, a lattice-type model is employed [6,17]. This lattice-type model can simulate failure behavior as well as overall load-deformation behavior. In the RC beams, overall failure is regarded as when the compressive zone cannot be further strained and crushes or the steel reinforcement ruptures in tension.

2. Numerical modeling

2.1. Lattice model

Lattice models have been widely used to simulate the brittle failure of materials [18–20]. In the most basic case, crack growth is modeled by removing (from the mesh) the element with the highest stress-to-strength ratio. The fracture is based on the maximum tensile stress that occurs in the outermost fiber of a frame

* Corresponding author. Tel.: +82 2 2123 2796; fax: +82 2 364 5300.
E-mail address: yunmook@yonsei.ac.kr (Y.M. Lim).

0958-9465/$ - see front matter © 2010 Elsevier Ltd. All rights reserved.
doi:10.1016/j.cemconcomp.2010.09.001

element due to moment and normal force at nodes i and j as shown in Eq. (1):

$$\sigma = \frac{\beta}{(1-\Omega)}\left(\frac{F}{A} + \alpha\frac{\max(|M_i|,|M_j|)}{W}\right) \quad (1)$$

where F is the axial force in the frame element, and M_i and M_j are the bending moments at nodes i and j of the frame element, respectively. Parameter A is the section area of a frame element with width b and depth h, and W is the element's section modulus ($bh^2/6$). Parameter Ω is a damage indicator initially set to zero for all elements; $\Omega = 1$ corresponds to removal of an element from the lattice (i.e., complete damage). The constant α is a parameter to control the influence of flexure on the fracture, and β is a parameter for scaling the element's effective stress to global stress levels. The significance of parameters α and β is discussed in Refs. [18–20].

The lattice model is based on iterations of linear elastic lattice behavior with introduced nonlinearities. Once an element is removed from the system, the solution is repeated linearly to reach another point on the load-deformation curve. As will be shown later, the model is able to realistically describe observed cracking patterns.

Cement-based materials such as concrete and DFRCC generally fail due to tensile cracking. In this study, therefore, the Axial Deformation Link Element (ADLE) model [6,17] was introduced to investigate the fracture behavior of the materials. This model considers only axial deformation between two neighboring points. At each load stage, the effective stress σ acting in each element is computed according to Eq. (1) when $\alpha = 0$. The ADL element with the highest ratio $R = \sigma/\sigma_f$ experiences a fracture event when $R \geqslant 1.0$, where σ is the axial stress in the element and σ_f is the tensile strength of the material. Internal element forces associated with this change are released, and both the element and system stiffness matrices reform. To model the macroscopic nature of the material and fracture process better, the stiffness of fracturing elements was gradually reduced via the damage parameter Ω depending on the component type. The ADLE model adopts post-peak softening to represent localization and account for energy consumption by the fracture process. This model reveals a realistic stress–strain response similar to that observed experimentally for concrete materials. For the reinforcement, it is modeled as elastic-perfectly plastic.

2.2. Constitutive relationships for DFRCC

A constitutive relationship for an ordinary DFRCC is shown in Fig. 1. The tensile stress increases linearly up to first cracking strength, f_t, after which DFRCC undergoes strain-hardening up to the ultimate tensile strength, $\beta_s f_t$. The ultimate tensile strength parameter β_s can change according to the characteristics of DFRCC. During strain-hardening, multiple micro-cracks form successively and become nearly equally spaced in parallel [6]. In the strain-softening region, transmitted tensile stress decreases after strain-hardening. During strain-softening, the "strain" is not uniquely defined, but depends on gauge length. Deformation at this stage is more appropriately described by crack opening displacement, and it begins to localize in the transition from a uniform deformation field (multiple cracking deformation) to the crack opening displacement of a single crack [6].

3. Behavior of a RC beam strengthened with DFRCC

To demonstrate the feasibility of the developed numerical program to RC structure, numerical simulation is carried out for four-point bending RC beam as shown in Fig. 2a. The material properties used in this simulation are same as those of an experiment [20]. The material properties of concrete used in this simulation are as follows: elastic modulus $E_c = 26.4$ GPa, first cracking strength $f_t = 2.8$ MPa, and fracture energy $G_F = 96.8$ N/m. The material properties for reinforcement used in this simulation are: elastic modulus $E_s = 200.0$ GPa and yield strength $f_y = 414.0$ MPa. Fig. 3 shows the experimental and numerical load–displacement responses for four-bending test. The numerical results are in good agreement with those of experiment in the pre-peak region and ultimate strength. The maximum displacements at failure stage, however, are different from experiment (30 mm) and numerical simulation (40 mm). The perfect bond assumption between concrete and rebar is one of the reasons and the modeling of compressive behavior in the lattice-type model might influence the maximum displacement.

To investigate the strengthening effect of DFRCC, numerical simulations are carried out for RC beams strengthened with a cover thickness of DFRCC and twice the cover thickness at the bottom tension section of the specimen (beams SC, SD) as shown in Fig. 2b. The material properties for DFRCC used in this simulation are: elastic modulus $E = 20.0$ GPa, first cracking strength $f_t = 2.5$ MPa, and ultimate tensile strength of 5.0 MPa ($\beta_s = 2.0$).

The load–displacement curves of SC and SD beams are presented in Fig. 4 together with the results for the control beam. The control beam, in this case, refers to a beam without the strengthening reinforcement of DFRCC. Whereas the initial stiffness of SC and SD beams is lower than that of the control beam, the peak load of the SC and SD beams is higher than that of the control beam, and it increase with the thickness of DFRCC. This is because the elastic modulus of DFRCC is smaller than that of concrete, but the ultimate tensile strength is higher. The maximum loads are 49.6 kN, 50.6 kN, 54.3 kN, and the displacements at failure are 40.6 mm, 45.6 mm, 54.6 mm for the control beam, SC, and SD, respectively. These results show increases by as much as

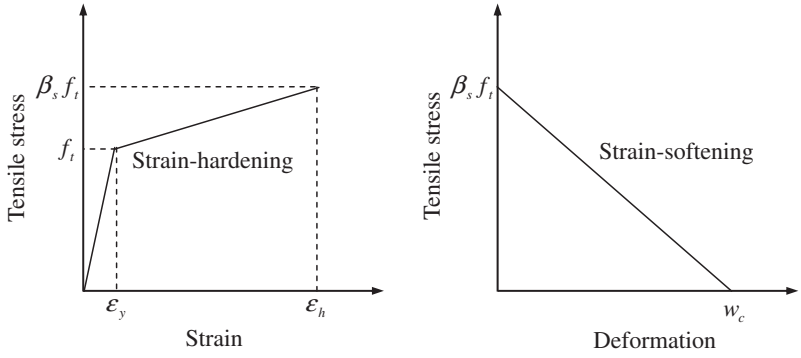

Fig. 1. Constitutive relationship of DFRCC.

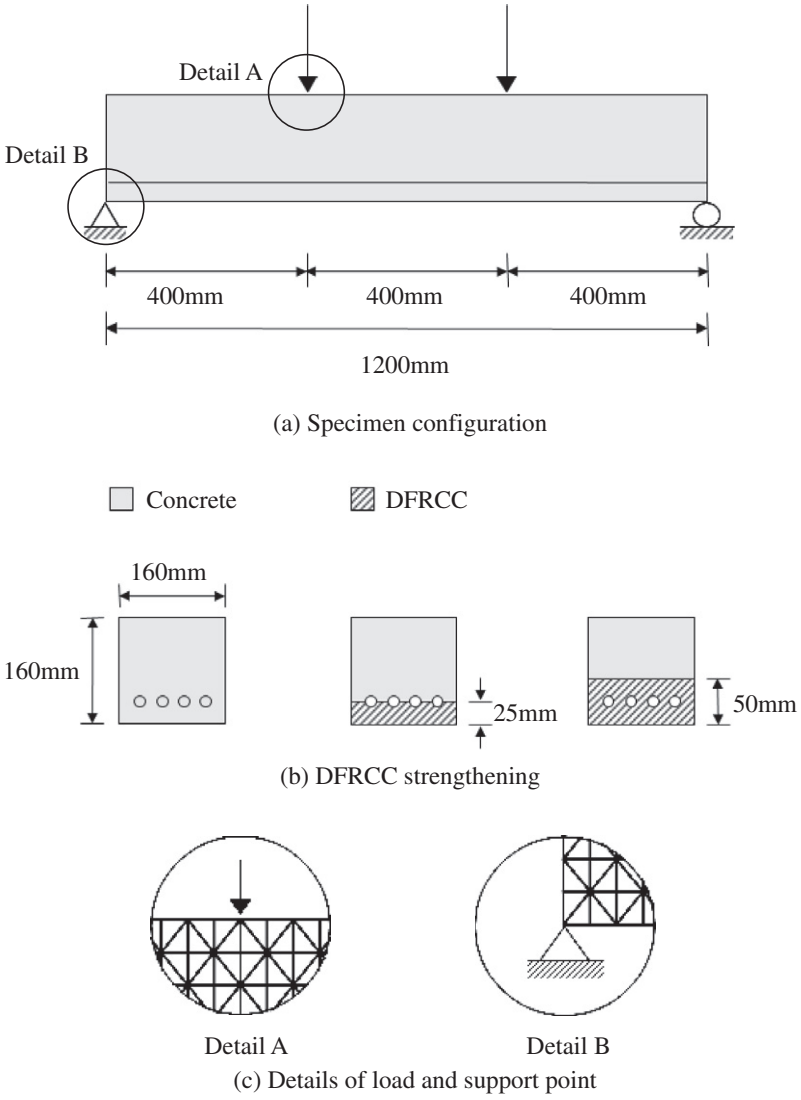

Fig. 2. Four-point bending specimen configuration and DFRCC strengthening.

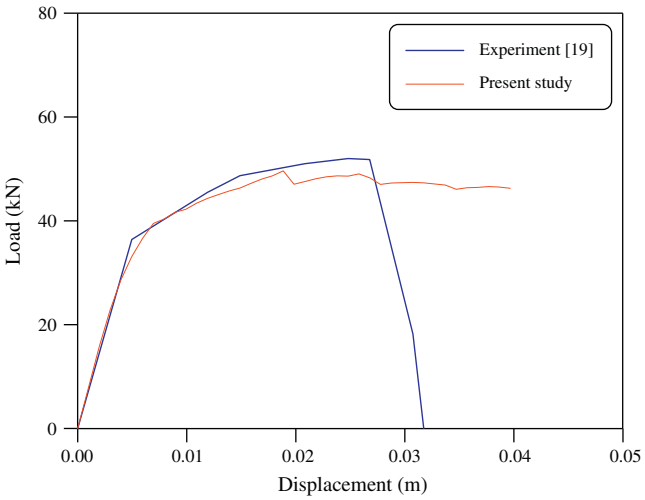

Fig. 3. Comparison of experimental and predicted load–displacement curve for RC.

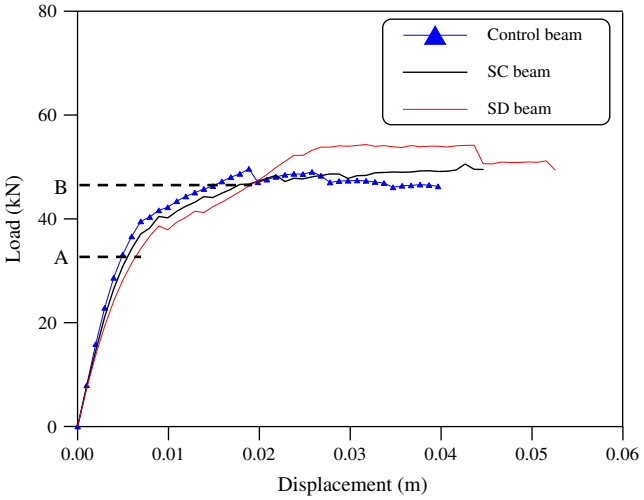

Fig. 4. Load–displacement curve of various DFRCC.

9.5% and 34.4% in the maximum load and the displacement at failure, respectively.

Fig. 5 shows the stress variation in the reinforcement of each beam. This is at the load level A of Fig. 4. The reinforcement stresses of SC and SD decrease considerably compared to the control beam. The maximum stress of SC decreases by 24.6% and that of SD decreases by 48.3% compared to the control beam. The results show that stress concentrations can be avoided in the reinforcement with DFRCC strengthening. It is important because the stress concentration may cause the yielding of reinforcement. The crack opening in the tension face is shown in Fig. 6 in order to investigate the crack controlling effects of DFRCC. This is at the point B of Fig. 4. The maximum crack opening of SC decreases by 75.2% and that of SD by 95.0% when compared with the control beam. This phenomenon is probably due to the initiation of multiple but finer cracks in the DFRCC. This damage-tolerant behavior delays flexural failure of the structure.

Fig. 7 shows the load–displacement curve, failure mechanism, and crack propagation for the SC beam. The failure mechanism and average crack width are compared with each loading step A, B, C, and D. The figure shows the crack propagation with each increased loading step. In the point A, small tension cracks on the tensile surface begin to form, and minor damage occurs at the interface. When the loading step is reached to the load level B (near the maximum load), multiple fine cracks develop into several major cracks due to crack localization in the concrete region. The maximum crack width is under 340 μm until the loading step of point C. In the loading step of point D, however, the maximum crack width is 2100 μm. The load–displacement curve and cracking behavior of the SD beam are shown to be similar to those of the SC beam.

4. Effects of DFRCC strain capacity

In this section, the behavior of the SC and SD beams will be studied with a variety of constitutive relations for DFRCC. A four-point bending simulation is carried out for the same specimen as shown in Fig. 2. Parametric studies are conducted on the strengthened RC beam with different strain capacities and strain-hardening slopes for DFRCC in order to investigate their effects on the overall load-deformation and cracking behavior. DFRCC is assigned the same ultimate tensile strength of 5.0 MPa, whereas the strain capacity is variably 1%, 2%, 3%, and

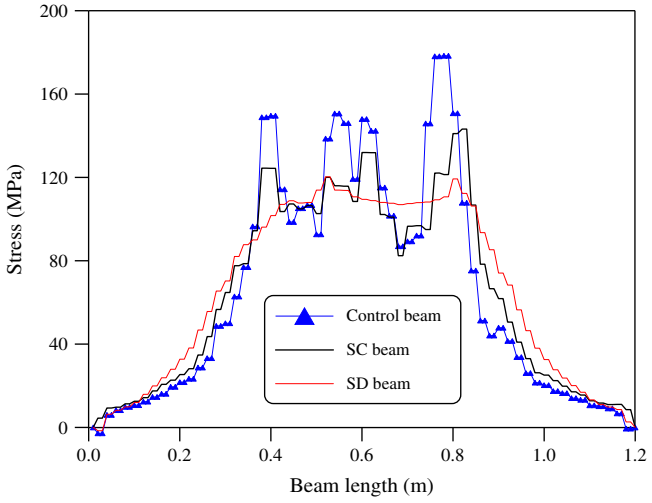

Fig. 5. Stress variation in the reinforcement of each beam at load level A in Fig. 4.

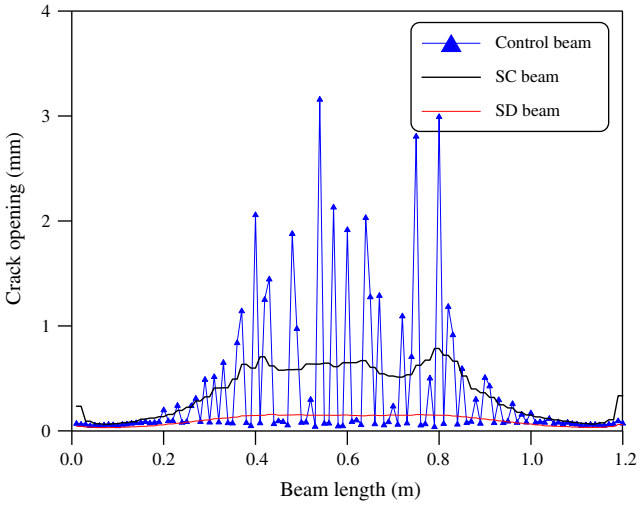

Fig. 6. Crack opening in the tension face of each beam.

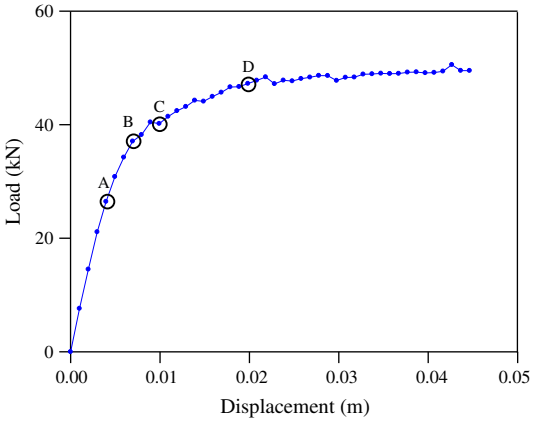

(a) Load-displacement curve

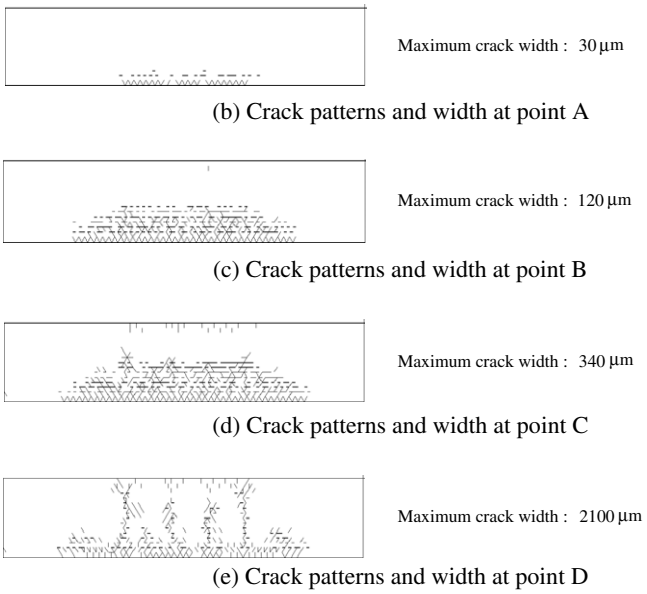

Fig. 7. Load–displacement curve, crack patterns and width of SC beam.

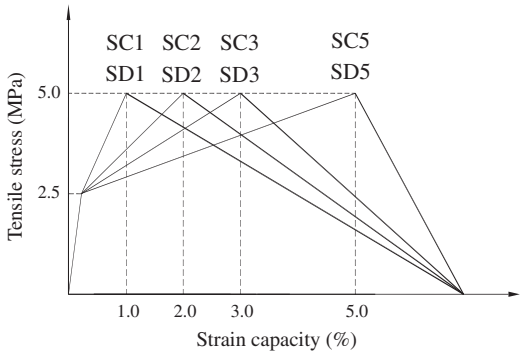

Fig. 8. Constitutive relations of DFRCC with different strain capacities.

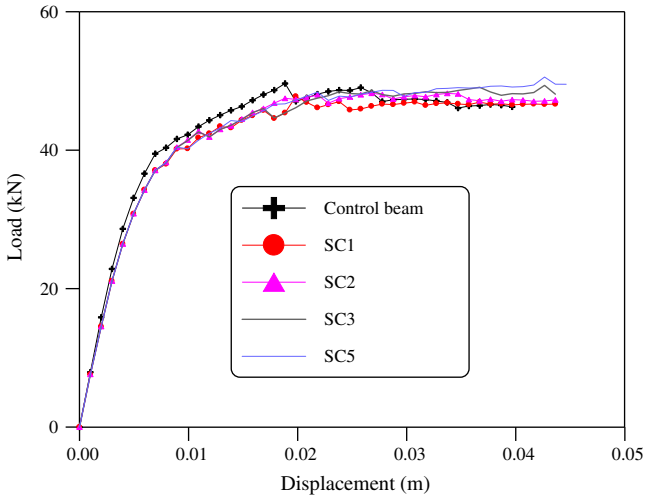

Fig. 9. Effect of different strain capacities on the load–deflection response for the group of SC beams.

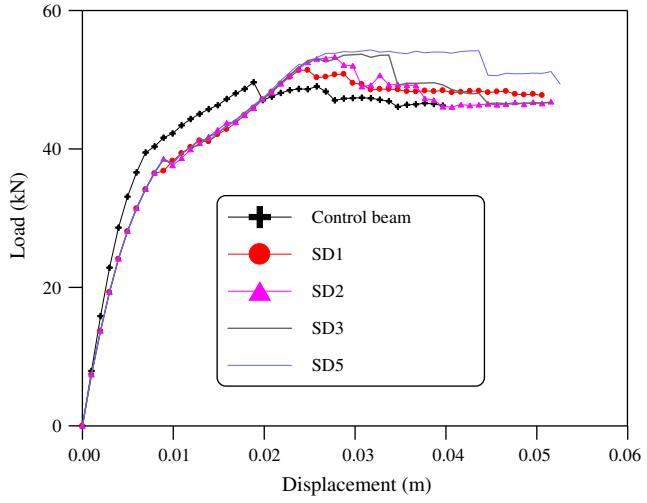

Fig. 10. Effect of different strain capacities on the load–deflection response for the group of SD beams.

5% with a different strain-hardening slope for each simulation, as shown in Fig. 8. Numerically simulated beams are classified into two groups. For the group of SC beams, beams are named SC1, SC2, SC3, and SC5, and SD beams are named SD1, SD2, SD3, and SD5, according to the percentage of strain capacity of the strengthening material.

The load–deflection responses are depicted in Figs. 9 and 10 for SC and SD beams, respectively. For the SC beams, the peak loads are 49.6 kN, 47.8 kN, 48.2 kN, 49.4 kN, and 50.6 kN, and the displacements at failure are 40.7 mm, 44.6 mm, 44.6 mm, 44.6 mm, and 45.6 mm for the control beam, SC1, SC2, SC3, and SC5, respectively. The peak loads are almost the same regardless of the strain capacity of DFRCC. On the contrary, the increase of ultimate displacements changes slightly as the strain capacity increases, up to 12.3% over the control beam in the case of SC5.

For the SD beams, the peak loads are 49.6 kN, 51.4 kN, 53.3 kN, 53.7 kN, and 54.3 kN for the control beam, SD1, SD2, SD3, and SD5, respectively. As the strain capacity of DFRCC increases, the peak loads have a tendency to increase as well. The peak load of SD5 increases by as much as 9.5% over the control beam. The displacements at failure are 40.7 mm, 51.6 mm, 52.6 mm, 52.6 mm, and 53.6 mm for the control beam, SD1, SD2, SD3, and SD5, respectively. The displacement at failure for SD5 increases by as much as 31.7% over the control beam. Comparing the SC and SD cases, the SD beams show better results for peak load and displacement at failure than the SC beams. In other words, the strengthening effect increases as the thickness of DFRCC increases.

5. Concluding remarks

In the present paper, a numerical model was developed to evaluate the behavior of RC beams under flexural loading. The model results are in good agreement with those of an experiment in the pre-peak region and ultimate strength. The numerical model has been used to estimate the structural performance of RC beams strengthened with Ductile Fiber Reinforced Cementitious Composites (DFRCC). The DFRCC is assumed to have a hardening behavior for tensile strains up to 5–6%. To investigate the strengthening effect of DFRCC, numerical simulations were carried out for four-point bending of RC beams strengthened with a cover thickness (and twice the cover thickness) of DFRCC within the extreme tensile zone of the specimen. The following conclusions have been reached from this modeling effort.

1. The maximum load carrying capacity and displacement at failure of DFRCC strengthened RC beams increase by as much as 9.5% and 34.4%, respectively, when compared with the control beam (without DFRCC strengthening).
2. Strengthening with DFRCC can also avoid stress concentrations in the reinforcement and delay flexural failure of the structure due to the damage-tolerant behavior of DFRCC. The maximum stress of reinforcement decreases by 24.6–48.3% with increasing DFRCC strengthening thickness. The maximum crack opening also decreases by 75.2–95.0% when compared with the control beam. Since the permeability is related to the cube of crack width, DFRCC strengthening might be also effective to prevent reinforcement from corrosion.
3. The parametric studies conducted on the strengthened RC beam with different strain capacities and strain-hardening slopes for DFRCC show that the SD beams provide better results for peak load at failure than the SC beams. In other words, the strengthening effect increases as the thickness of DFRCC increases. It is seen that the peak load of reinforced concrete beams increases significantly according to increased ductility of the DFRCC strengthening layer.

Acknowledgement

This research was supported by a grant from the Gas Plant R&D Center funded by the Ministry of Land, Transportation and Maritime Affairs (MLTM) of the Korean government.

References

[1] Niu HD, Karbhari VM, Wu ZS. Diagonal macro-crack induced debonding mechanisms in FRP rehabilitated concrete. Compos Part B: Eng 2006;37:627–41.
[2] Bhargava K, Ghosh AK, Mori Y, Ramanujam S. Modeling of time to corrosion-induced cover cracking in reinforced concrete structures. Cem Concr Res 2005;35:2203–18.
[3] Elbadry M, Elzaroug O. Control of cracking due to temperature in structural concrete reinforced with CFRP bars. Compos Struct 2004;64:37–45.
[4] Nishino M, Aoki T. Nonlinear analysis and damage monitoring of a one-sided patch repair with delamination. Compos Struct 2006;73:423–31.
[5] Lim YM. Interface fracture behavior of rehabilitated concrete infrastructures using engineered cementitious composite. PhD thesis, University of Michigan, Ann Arbor; 1996.
[6] Shin SK, Kim JJH, Lim YM. Investigation of the strengthening effect of DFRCC applied to plain concrete beams. Cem Concr Compos 2007;29:465–73.
[7] Kamada T, Li VC. The effect of surface preparation on the fracture behavior of ECC/concrete repair system. Cem Concr Compos 2000;22:423–31.
[8] Li VC, Horii H, Kabele P, Kanda T, Lim YM. Repair and retrofit with engineered cementitious composites. Eng Fract Mech 2000;65:317–34.
[9] Li VC, Wang S, Wu C. Tensile strain-hardening behavior of polyvinyl alcohol engineered cementious composite. ACI Struct J 2001:483–92.
[10] Li VC. From micromechanics to structural engineering—the design of cementitious composites for civil engineering applications. JSCE J Struct Mech Earthquake Eng 1993;10(2):37–48.
[11] Lim YM, Li VC. Durable repair of aged infrastructure using trapping mechanism of engineered cementitious composites. Cem Concr Compos 1997;19(4):373–85.
[12] Matsui S. Technology developments for bridge decks—innovations on durability and construction. Kyouryou To Kiso 1997;97:84–92.
[13] Li VC, Kanda T. Engineering cementitious composites for structural applications. ASCE Mater J Civ Eng 1998;10(2):66–9.
[14] Kamada T, Li VC. The effects of surface preparation on the fracture behavior of ECC/concrete repair system. Cem Concr Compos 2000;22(6):423–31.
[15] Kamal A, Kunieda M, Ueda N, Nakamura H. Evaluation of crack opening performance of a repair material with strain hardening behavior. Cem Concr Compos 2008;30(10):863–71.
[16] Kobayashi K, Iizuka T, Kurachi H, Rokugo K. Corrosion protection performance of high performance fiber reinforced cement composites as a repair material. Cem Concr Compos 2010;32(6):411–20.
[17] Lim YM, Shin SK, Kim MK. A study on the effect of externally bonded composite plate-concrete interfaces. Compos Struct 2008;82:403–12.
[18] Schlangen E, van Mier JGM. Experimental and numerical analysis of micromechanisms of fracture of cement-based composites. Cem Concr Compos 1992;14:105–18.
[19] Schlangen E, van Mier JGM. Simple lattice model for numerical simulation of concrete materials and structures. Mater Struct 1992;25:534–42.
[20] Hussain M, Sharif A, Basunbul IA, Baluch MH, Al-Sulaimani GJ. Flexural behavior of precracked reinforced concrete beams strengthened externally by steel plates. ACI Struct J 1995;92:14–22.